Corrosion prevention of mild steel in a simulated concrete medium by the electro-application of a polyaniline coating

Mouna Mrad[a,b*], Leila Dhouibi[a]

[a]*Unité de Recherche Mécanique-Energétique-ENIT, Equipe de Recherche, COPROMET, Ecole Nationale d'Ingénieurs de Tunis (ENIT), Tunis El Manar University, le Belvédère 1002 Tunis, Tunisia.*
[b]*Institut National des Sciences Appliquées et de Technologie (INSAT), Carthage University, 1080 Tunis, Tunisia.*

(Received: 03 May 2017, accepted: 14 June 2018)

Abstract: Polyaniline (PANI) film was successively electrodeposited onto mild steel (MS) by cyclic voltammetry from oxalic acid solution. The anticorrosion performance of PANI was investigated in a simulated concrete medium consisted on a filtered saturated lime solution contaminated with 0.5 M NaCl. Corrosion studies were carried out using standard electrochemical methods, electrochemical impedance spectroscopy (EIS) and SEM analysis. PANI proved high inhibition efficiency against MS corrosion. The anticorrosive action of PANI was related, on one hand, to its catalytic behaviour in the oxides layer healing mechanism taking place at the polymer/MS interface and, on another hand, to its physical barrier property against diffusion of corrosives species toward MS surface.

Keywords: PANI, electropolymerization, MS, simulated concrete medium, corrosion.

INTRODUCTION

Reinforcement steel was widely used in reinforced concreted infrastructures. However, corrosion of reinforcement steel was the main reason of concrete structures deterioration [1-2]. The corrosion processes were dependant on environmental factors such as marine environment. Under normal conditions, reinforcing steel surface could be protected from corrosion through the formation of an iron oxides layer [3]. Nevertheless, once the chlorides concentration at the steel/ concrete interface reached critical values, a breakdown of passivity state took place and the reinforcing steel was subject to a localized corrosion [4].

In order to protect reinforcement steel against corrosion, a variety of technologies were tested namely patch repairs [5], coatings [6], sealing and membranes for concrete surface [7], special steel bar (stainless steel bar, epoxy coated steel reinforcement) [8], cathodic protection [9] and use of corrosion inhibitors [10, 11].

Although, to our knowledge, until today, performances of conducting polymers against corrosion of reinforcement mild steel have not been investigated.

Since their revolutionary discovery, electro-conducting polymers (CP) have not stopped to attract attention of researchers in many industrial and technological fields such as energy storage systems [12], sensors [13], electronics devices [14], etc.

Several techniques were applied to synthesis electroconducting polymers [15-17]. The most commonly technique was the electrochemical oxidative polymerization: electropolymerization [18, 19]. This procedure allows control of the different CP properties namely: uniformity, thickness, porosity, etc. Moreover, it presents the advantage of simultaneous polymerization and deposition of polymer coating onto metallic surfaces [18, 19].

The possibility of electrochemical deposition of conducting polymer onto active metals (Fe, Al, Ti, etc) has opened up another important technological area of corrosion protection [18-21]. Indeed, resistance enhancements of iron and ferrous alloys against corrosion using conductive polymers have

* Corresponding author, e-mail address : mouna.mrad@yahoo.fr

been reported [20-22]. Among numerous known CP, polyaniline (PANI) was the most promising [22].

Several mechanisms have been proposed to explain effectiveness of PANI [25-28]. Thile et al. suggested an anodic galvanic protection mechanism in which PANI acted as an efficient oxidiser to maintain the passivation state of the metallic substrate [21]. Camalet et al. considered that PANI behaved as a physical barrier preventing aggressive species diffusion towards the metallic surfaces. Moreover, they reported that CP reacted as polymeric inhibitors lowing the degradation kinetic of metal substrate [22]. All protection process interpretations reported the dependence of CP anticorrosion performance on the metallic substrate/polymer interface state [20-24].

The electrodeposition possibility of the conducting polymers and its success depended on thermodynamic data. In fact, for certain active substrates, the metallic dissolution occurred before the monomer oxidation and the electropolymerization potential start was in the region of metal activity. Hence, the metal activity was able to retard, to inhibit the monomer oxidation and therefore to hinder the polymeric film formation [22-25]. Consequently, to success the electroelaboration of CP films on active electrodes, it was necessary to find electrochemical conditions able to decelerate the metal dissolution rate without preventing monomer oxidation and further its electropolymerization [25].

Numerous studies considered that electrogeneration of PANI on mild steel needed an aqueous acid electrolyte [26, 27].

The present study aimed to coat electrochemically the mild steel (MS) with PANI film from an oxalic acid solution containing aniline. The anticorrosion performance of PANI was examined in a lime saturated solution contaminated by chlorides (0.5 M NaCl) (pH=11.9). This medium has been proposed to simulate the interstitial conditions of the concrete used in the marine construction industry. Therefore, our work could be considered as the first investigation on the behaviour of MS coated with PANI against corrosion once it was embedded in cement mortar specimens exposed to chlorides.

EXPERIMENTAL

1. Metallic substrate

The working electrodes were prepared from cylindrical MS bars with a section of 0.193 cm^2 provided by Tunisian Iron and Steel Company. The elemental chemical composition of the mild steel electrode was summarized in Table I. MS bar was connected to a copper wire and was coated with a cold polymerizable resin casing (Fig. 1).

Table I. Chemical composition of mild steel

Element	Content (wt.%)
Mn	0.089
C	0.22
Si	0.24
P	0.046
S	0.016
Fe	balance

Prior to each experiment, electrodes surfaces were mechanically polished with abrasive papers (400-1200 mesh) on a Buehler polishing table and carefully washed with distillated water.

In order to remove surface oxides, electrodes were cathodically polarized in the electrochemical cell (see next section) during 5 min (the sweep rate = 25 mV/min) in 0.1 M sodium carbonate solution (pH=11.1). Then, MS electrodes were washed with distillated water and transferred immediately to the appropriate electrolyte.

2. Electrochemical cell

A conventional single-compartment three-electrode cell was used all electrochemical experiments (Fig. 1). All potentials were referred

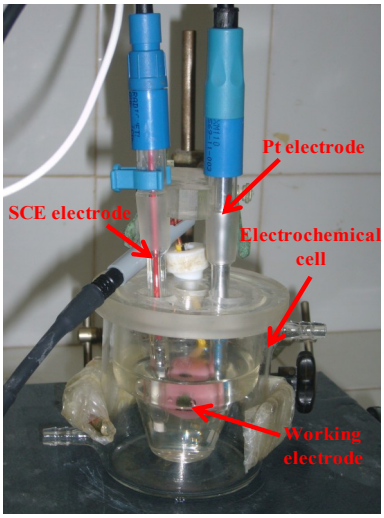

Figure 1: The electrochemical cell used for all electrochemical experiments

to a saturated calomel electrode (SCE) ($Hg/Hg_2Cl_2/KCl_{saturated}$; E= −0.2415 V/ENH). A platinum wire was used as a counter electrode.

3. Chemicals

All chemicals were of the highest quality commercially available. Aniline was purchased from Aldrich. Oxalic acid, sodium carbonate and dihydroxyde of calcium were supplied by Merck. Sodium chloride was obtained from Fluka.
Aniline was distilled under reduced pressure before use. The others chemical products were used as received without further purification.

4. Electrodeposition of PANI onto MS surface

The electropolymerization of aniline was carried out from an aqueous solution containing 0.1 M aniline + 0.3 M oxalic acid ($C_2H_2O_4$) (pH=1.7).
It was performed by cyclic voltammetry with a total scan number of 25 cycles and a scan rate of 10 $mV.s^{-1}$. Details of the potential range will be discussed in the next section. Cyclic voltammetry was carried out using Taccusel potentiostat-galvanostat type PGP201 piloted by an electrochemical software type Voltmaster 4.

5. Corrosion studies

Corrosion studies namely (i) evolution of open circuit potential (E_{ocp}), (ii) potentiodynamic polarization technique and (iii) electrochemical impedance spectroscopy (EIS) were conducted in an aerated lime saturated and filtered solution ($Ca(OH_2)$) containing chlorides (0.5 M NaCl). The pH of the corrosive medium was estimated at 11.9.
Polarization curves were performed using the same experimental equipment for PANI synthesis. Experiments were carried out after 30 min immersion in the aggressive medium by cycling the potential from ±0.05 V/SCE vs. E_{ocp} to higher anodic and cathodic potentials values with a scan rate of 25 $mV.min^{-1}$.
Tafel regions were analyzed from the anodic and the cathodic polarization curves using NOVA1.11 software from Metrohm.
EIS data were collected at open circuit potential for different immersion times. The equipment consisted on a Solarton apparatus with a FRACOM software for plotting impedance by controlling the analyser of transfer function. The perturbation voltage for EIS measurements was 10 mV and the frequency range went from 65 kHz to 10 mHz with 7 points/decade.

6. Characterization techniques

Morphological property of PANI was assessed by scanning electron microscopy (SEM) using a Hitachi Model S-2400 microscope with an acceleration beam of 25 keV. Furthermore, to observe surfaces states, optical images were done using an optical microscope Nikon SMZ25.
PANI coating was analyzed by UV-Vis analysis conducted using a Shimadzu's SolidSpec-3700/3700DUV spectrophotometer, in a range of 200-900 nm.

RESULTS AND DISCCUSSION

1. Electrodeposition of PANI onto MS surface

In order to choose the suitable potentials range for PANI nucleation and growth, it was necessary to start by examining the stability and the behaviour of MS in free-monomer and containing aniline electrolytes (Fig. 2 and Fig. 4 respectively).
Figure 2 illustrates the mild steel behaviour in 0.3 M acid oxalic solution. The cyclic voltam-mogram was recorded from -0.70 to +1.60 V/SCE. The anodic sweep displayed a peak (P_1) at -0.28 V/SCE. Such activity was related to a metallic oxidation/ passivation process. In fact, the passivation was based on the formation of insoluble iron (II) oxalates complexes [28,29]. The associated mechanism could be described as follow:

$$Fe \rightleftarrows Fe^{2+} + 2e \qquad \text{(Eq.1)}$$

$$Fe^{2+} + C_2O_4^{2-} \rightleftarrows Fe(C_2O_4) \downarrow \qquad \text{(Eq.2)}$$

At high potentials (between +0.50 and +1.30 V/ SCE), a slightly current density increase appeared

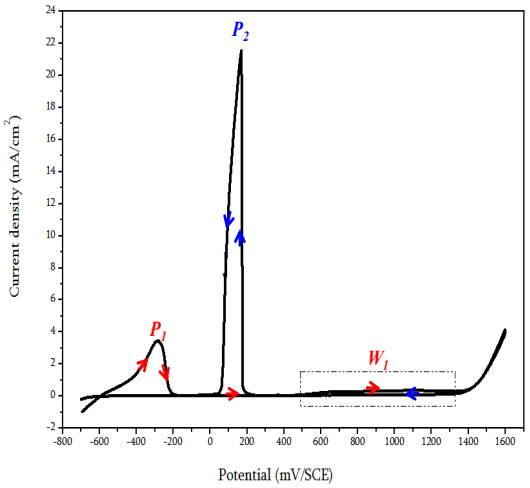

Figure 2: Cyclic voltammogram obtained for MS in 0.3 M oxalic acid free monomer solution (pH= 1.7) (v = 10 $mV.s^{-1}$)

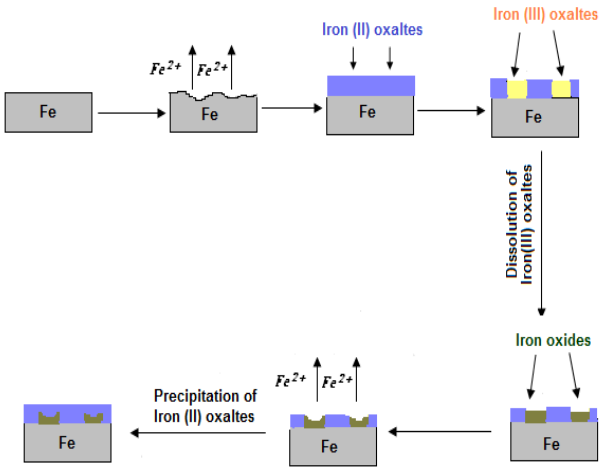

Figure 3: Modifications of MS surface during CV in the oxalic acid solution

(W_1). It was attributed to the conversion of iron (II) oxalates, already formed, into iron (III) oxalates compounds (see Eq.3) [28, 29]. The dissolution of iron (III) oxalates was accompanied by the formation of iron oxides (Fe_2O_3) which reformed the passivation layer [28, 29].

Iron (II) oxaltes ⇄ Iron (III) oxaltes + e^- (Eq.3)

The dissolution of MS took place at around +1.40 V/ECS.

The reverse scan was characterized, at +0.17 V/SCE, by a sharp oxidation peak (P_2) attributed to the repassivation of the mild steel electrode.

According to Mengoli and Musiani [28], the iron oxide layer underwent an aggressive attack during the reverse scanning which was inhibited by a precipitation of iron (II) oxalates on the surface.

Figure 3 illustrates the different mild steel surface modifications occurred during the cyclic polarization in 0.3 M oxalic acid [29].

Figure 4a presents the first four successive voltammograms, recorded from -0.70 to +1.60 V/SCE in 0.3 M oxalic acid solution containing 0.1 M aniline.

In the first voltammogram, peaks P_1 and P_2 observed in a pure oxalic acid solution were still present. Noted that peaks current densities decreased compared with those obtained in free-monomer solution. This decrease was explained by the inhibitor effect of aniline on metallic dissolution. Moreover, the first voltammogram showed an oxidation aniline peak at +1.40 V/SCE.

The second voltammogram revealed a new oxidation peak (B_2) localized between +0.20 and +0.45 V/SCE and a reduction wave (C_2) at +0.37 V/SCE. These responses were related to the development of a thin PANI film on the MS surface. The same voltammogram exhibited the disappearance of peak P_1 and a slight shift towards the cathodic domain coupled to a dramatic current decrease for peak P_2 (designated D_2 in presence of aniline).

The third and the fourth voltammograms showed the same pattern with a slightly shift of peaks B and C to more positive and more negative values respectively. Moreover, voltammograms showed

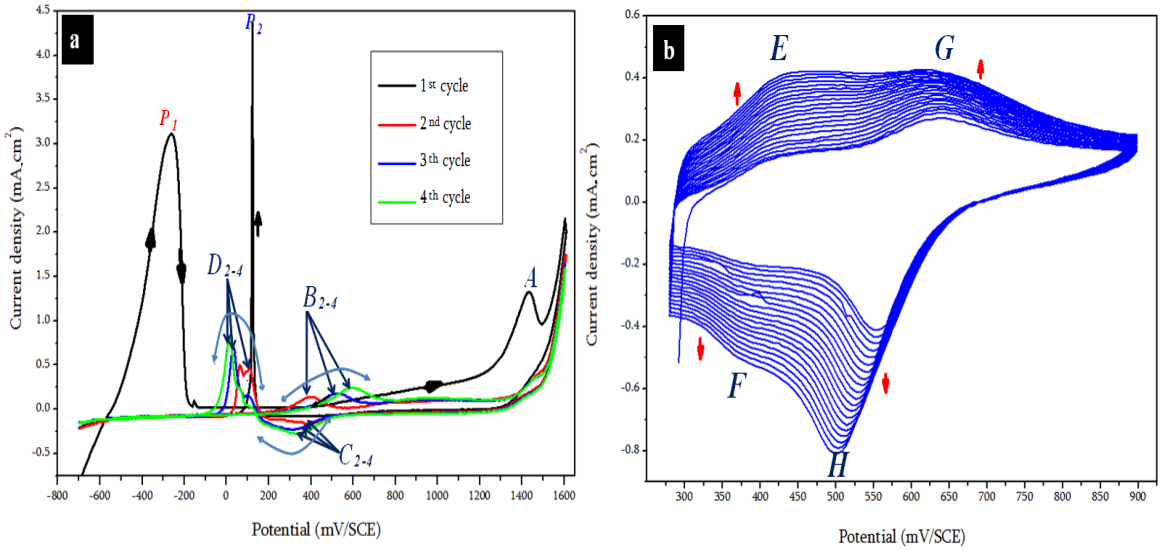

Figure 4: Cyclic voltammograms recorded for MS in 0.3 M oxalic acid + 0.1 M aniline solution: (a) the five first cyclic voltammograms, (b) the 20 last cycles voltammograms describing PANI growth (v = 10 mV.s^{-1})

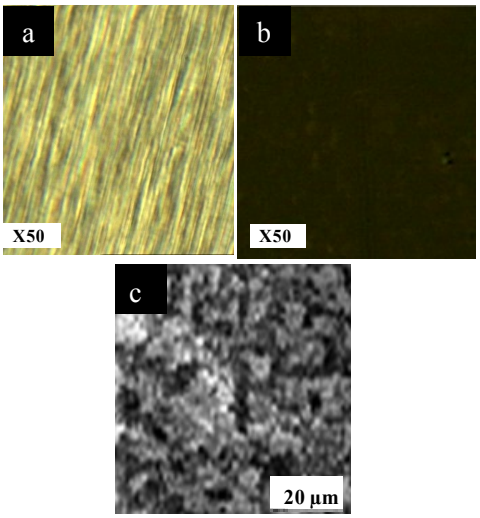

Figure 5: (a) and (b) Metallographic observations of bare and coated mild steel (X 50) respectively, (c) SEM micrographs of a MS surface covered with PANI

the persistence of peak *D* which was not suitable for the formation of a uniform, adherent and non-porous PANI film onto the MS surface.

For better PANI growth, electropolymerization of aniline was performed following several steps:

(1) In order to allowed the metallic passivation and the aniline oxidation, the first cycle was carried out between -0.70 and +1.60 V/SCE.

(2) The following four voltmmograms were realized in a potential range of +0.28/+1.60 V/SCE and this to ensure that the entire amount of aniline species has been oxidized. In fact, these cycles allowed nucleation of PANI in absence of any metallic alteration. Noted that voltammograms revealed the absence of peak (D) and the presence of B and C peaks (not shown) which indicated on the formation of PANI.

(3) Finally, the last 20 cycles were performed between +0.28 and +0.90 V/SCE (Fig. 4b). These cycles promoted the growth of PANI.

PANI growth voltammograms shown in Fig. 4b, presented two redox pair peaks (E-F) and (G-H) at (+0.42; +0.34 V/SCE) and (+0.64; +0.55 V/SCE) respectively. Current densities values increased subsequently by increasing the cycle's number proving thus, a film growth. The redox pair peaks (G-H) described the interconversion reaction between the half oxidized PANI form and the 100% oxidized form [30]. The first pair peaks (E-F) having the lowest current densities, was attributed to the formation of secondary products [30, 31].

In fact, in order to observe the complete PANI electroactivity, interval polarization must begin from -0.20 V/SCE [30] which was not possible regarding to metallic activity.

Optical observations showed that the uncoated MS sample (Fig. 5a) demonstrated clearly the fine polishing groves which disappeared after the electrodeposition essay indicated on the success of PANI deposition onto MS (Fig. 5b).

2. Characterization of PANI coating

As could be seen from SEM micrograph of the coated MS surface, PANI film presented a cauliflower structure (Fig. 5c).

Figure 6 displays UV-Vis spectrum of PANI. It depicted three bands characteristic of the conductive emeraldine salt state (ES) of PANI [32, 34].

The first one (200-400 nm) was assigned to $\pi \rightarrow \pi^*$ transition of benzenoid system. The second band (400-700 nm) was attributed to $n \rightarrow \pi^*$ transition characterizing the charge transfer between a quinoid and a benzenoid cycle. The third band ($\succ$ 700 nm) was associated to the presence of polarons resulting from doping [33, 34].

3. Corrosion tests

E_{ocp} evolutions of the PANI coated and the bare MS electrodes immersed in $Ca(OH_2)_{sat}$/0.5 M NaCl mixture were given in Fig. 7.

The initial E_{ocp} value of bare MS was estimated at -1.10 V/SCE. It increased rapidly over 20 min immersion to reach -0.60 V/SCE. After 1 h immersion, E_{ocp} value was evaluated at -0.58 V/SCE (Fig. 7a).

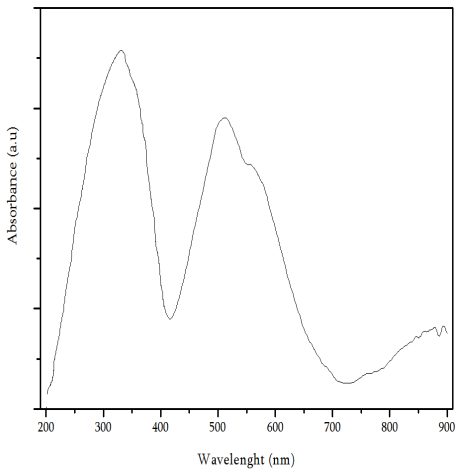

Figure 6: UV-vis spectrum of PANI

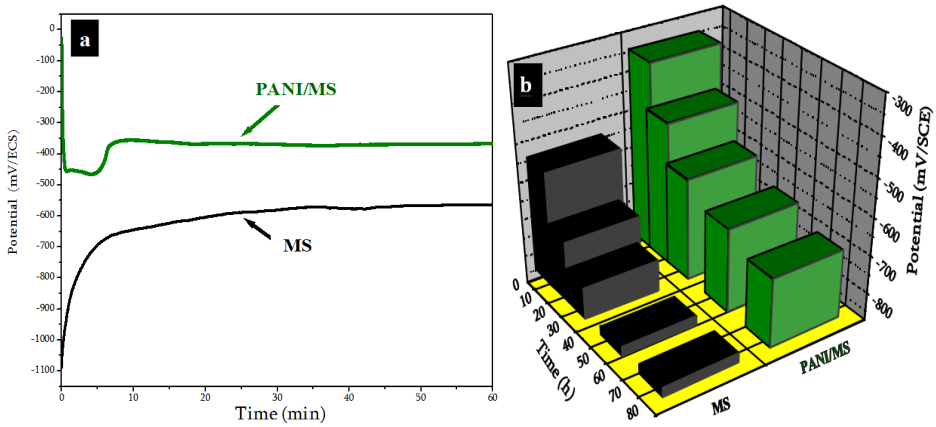

Figure 7: E_{ocp} evolution (a) during the first hour immersion and (b) as function of immersion time in a lime saturated solution/0.5M NaCl

Once covered with PANI, the initial E_{ocp} value of MS electrode was recorded at -0.03 V/SCE. This result proved the effective barrier property of polyaniline coating.

During the first immersion stage, E_{ocp} decreased dramatically and reached a value of -0.45 V/SCE after 1 min immersion. After 6 min, it started to increase and kept a constant value of -0.34 V/SCE. By extending the immersion time in $Ca(OH_2)_{sat}$/0.5 M NaCl, E_{ocp} values of the covered MS electrode remained higher than those recorded for the bare mild steel (Fig. 7b). E_{ocp} results proved that PANI coating was efficient against corrosion of mild steel in a lime saturated solution contaminated by 0.5 M NaCl.

After 24 h immersion, MS surfaces were observed. The uncoated MS surface was degraded and covered with corrosion products (Fig. 8a and 8c). However, no aggressive effect was observed for MS covered with PANI film which was still adherent to the metallic surface (Fig. 8b and 8c).

Potentiodynamic polarization curves were registered after 30 min immersion in the corrosive solution (Fig. 9). Table II gives the corrosion parameters extrapolated from curves of Fig. 9 namely corrosion current density (i_{corr}), corrosion and pitting potentials (E_{corr} and E_{pit} respectively), anodic and cathodic slopes (β_a and β_c respectively) and polarization resistance (R_p). R_p was estimated by the following equation [35]:

$$R_p = \frac{\beta_a \times \beta_c}{2.303\, i_{corr} \times (\beta_a + \beta_c)} \qquad (R.1)$$

The anodic behavior of MS specimen had been strongly affected by the application of PANI (Fig. 9a). The coated electrode showed nobler E_{corr} and E_{pit} values and lower corrosion and anodic current densities (Table II). Moreover, application of PANI has expanded the passivation plateau since ΔE_{corr}-E_{pit} increased.

Fig. 9b showed a dramatically decrease of the cathodic current densities once PANI was electrodeposited onto MS surface.

Tafel slopes presented different values for both tested specimens. The higher ones were calculated for the coated MS. Such difference highlighted change in both metallic dissolution and oxygen reduction mechanisms which seemed decelerated by application of PANI coating.

Concerning the linear polarization resistance, bare steel delivered a value quit lower than the one

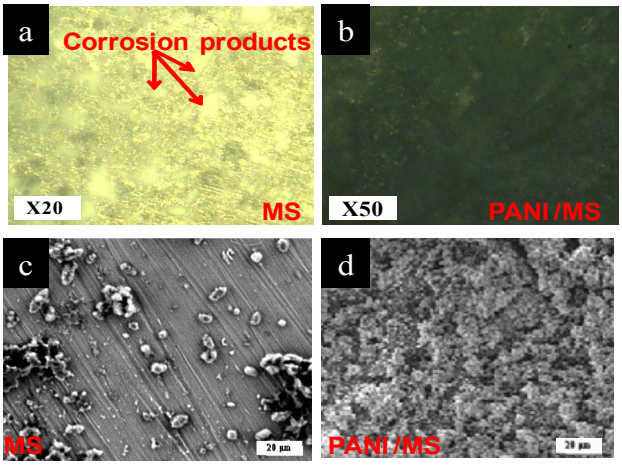

Figure 8: Optical (a,b) and SEM (c,d) observations of MS surfaces after 24 h immersion in a lime saturated solution containing 0.5 M NaCl: (a,c) Bare MS, (b,d) MS coated with PANI

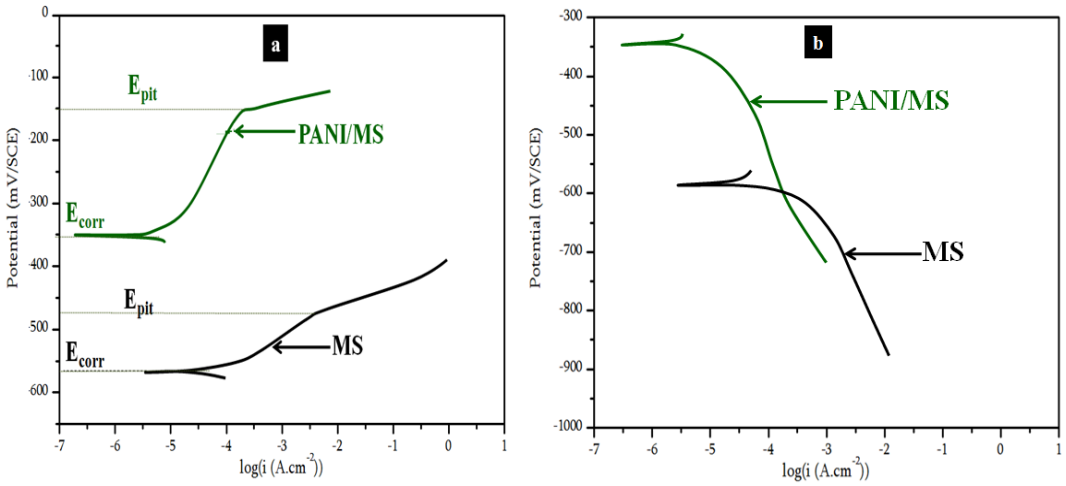

Figure 9: (a) Anodic and (b) cathodic polarization curves obtained for bare and coated MS electrodes recorded after 30 min immersion in $Ca(OH_2)_{sat}$/0.5M NaCl (v = 25mV.min^{-1}

obtained for coated steel. Based on the assumption that polarization resistance was inversely proportional to corrosion current density [35], it could be concluded that MS corrosion rate has decelerated in presence of PANI.

Polarization results were in agreement with the E_{ocp} ones. They proved an anticorrosion performance of PANI against corrosion of mild steel. In fact, the percentage inhibition efficiency (η (%)) accorded to PANI coating was estimated at 92.57 (%). Noted that η (%) was calculated using the equation depicted below [36]:

$$\eta\% = \frac{i_{corr}^{MS} - i_{corr}^{coat}}{i_{corr}^{MS}} \times 100 \qquad \text{(R.2)}$$

where:

i_{corr}^{coat} : corrosion current density of the coated MS (A.cm^{-2});

i_{corr}^{MS} : corrosion current density of the uncoated MS (A.cm^{-2}).

EIS experiments were carried out in $Ca(OH_2)_{sat}$/0.5 M NaCl for MS specimens coated or not with PANI. EIS data were presented in terms of Bode plots (Fig. 10). EIS spectra of bare MS were shown for comparison.

After 2 h immersion, $|Z|_{0.02\ Hz}$ (impedance modulus value estimated at 0.02 Hz) was 8.01 × 10 ^{6} Ω.cm^2 for the coated sample being more than 3 orders higher than that of bare MS (1.023 × 10^3). $|Z|_{0.02\ Hz}$ dropped progressively as function of immersion time. After 72 h immersion, $|Z|_{0.02\ Hz}$ failed to 8.91 × 10^4 Ω.cm^2 and 446.58 Ω.cm^2 for the coated and bare MS respectively.

Since low-frequency impedance ($|Z|_{LF}$) values of electrodes exposed to an aggressive medium indicate on the overall resistance of films [37], it was evident from $|Z|_{0.02\ Hz}$ data (in accord with the previous corrosion tests results) that the resistance of mild steel against corrosion in $Ca(OH_2)_{sat}$/0.5 M NaCl solution was improved by application of PANI coating.

The anticorrosion performance of PANI could be connected with its barrier property and redox behavior [38, 39].

By dispersion forces as well as hydrogen bonds [40], PANI film adsorbed on MS surface. It acted as an organic barrier between MS and the corrosive medium.

Indeed, PANI destabilized the local equilibrium of electrical charge between the anodic and the cathodic sites (Fig. 11a).

By prolonging the immersion time, it was expected that corrosion process accelerated following

Table II: Corrosion parameters extrapolated from Fig. 9

	Bare MS	**PANI/MS**
E_{corr} (V/SCE)	-0.561	-0.353
E_{pit} (V/SCE)	-0.472	-0.05
i_{corr} (A.cm^{-2})	1.07 × 10^{-4}	7.94 × 10^{-6}
β_a (V. dec^{-1})	224.49	734.22
β_c (V. dec^{-1})	53.08	688.25
Rp (Ω.cm^2)	174.21 × 10^3	19.42 × 10^6

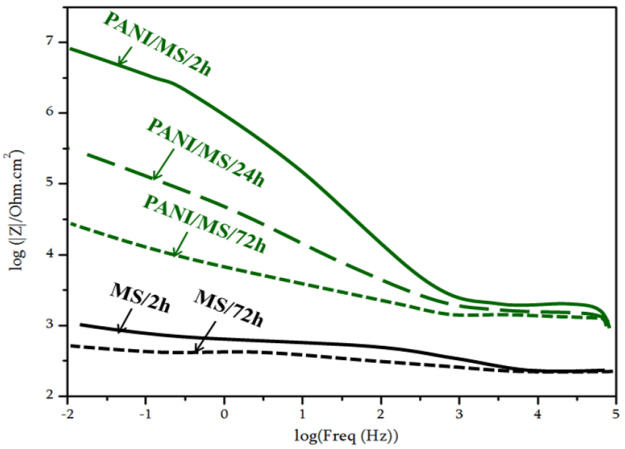

Figure 10: Bode plots obtained in $Ca(OH_2)_{sat}$/0.5M NaCl solution for MS

corrosive species uptake and hence, a loss of PANI adhesion and creation of defects in the coating network took place. However, EIS results revealed that even if PANI lost its barrier effect, it has been able to keep its anticorrosion performance. This was in agreement with the work of Pud et al. [41] having proved that in presence of defects artificially introduced into PANI coated mild steel, the reduction of corrosion rate remained significant.

Hence, it was assumed that to protect mild steel, PANI film did not react only by its barrier effect.

E_{corr} increase and i_{corr} decrease proved by the potentiodynamic polarization experiments were generally related to the formation of a passivation layer [42]. Based on the models proposed by Kinlen et al. [43] and Wesseling et al. [44], it was suggested that once PANI was presented in its ES state (according to UV-vis analysis), it participated on the formation of iron oxides due to its redox properties following the passivation mechanism given in Fig. 11b.

Catalytic efficiency of PANI coating included various events at the metal/coating/solution system [39]. In fact, at the bottom of PANI pores, the dissolution of iron was accompanied by PANI reduction. Such phenomenon produced a freshly oxides layer involved, the healing of oxides layer on mild steel surface.

Moreover, we suggested that the reaction of O_2 reduction translated to PANI-ES/electrolyte interface (Fig. 11c). It was proposed that PANI (ES) consumed the produced OH^- ions mechanism according to Eq.4 [22, 45].

$$Pani\text{-}(ES)/C_2O4_2^{2-} + OH^- \rightarrow Pani\ (EB) + H_2O + C_2O4_2^{2-} \quad (Eq.4)$$

The reduction of PANI-ES offered a buffer character to the polymer/MS interface which stabilized the oxides layer formed at the metallic surface and reduced the cathodic detachment of PANI [45].

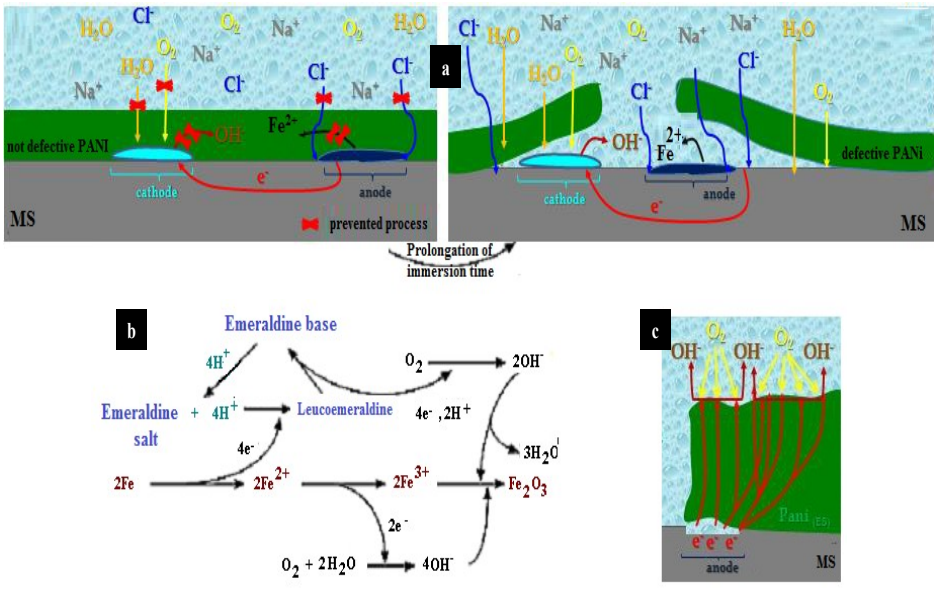

Figure 11: Schematic design of: (a) the barrier action of PANI, (b) the passivation mechanism involving the catalytic action of PANI, (c) the translation of oxygen reduction reaction on PANI-ES/electrolye interface

CONCLUSION

Polyaniline was successfully electrodeposited in its conductive state (ES) on mild steel by cyclic voltammetry from an $H_2C_2O_4$ solution. PANI presented a noticeable efficiency against corrosion of mild steel in a lime saturated solution contaminated by 0.5 M NaCl. The anticorrosion performance of PANI found explication on its barrier and redox properties. In fact, PANI prevented the diffusion of aggressive species toward MS surface, on one hand, and catalyzed the healing of oxides passivation layer on another hand.

REFERENCES

[1] D. A. Hausmann, Mater. Prot.,**1967**, *6*, 19-23
[2] A. M. Vaysburd, P. H. Emmons, Constr. Build. Mater., **2000**, *14*, 189-197
[3] G. Bikulcius, O. Girciene, V. Burokas, Rus. J. Appl. Chem., **2003**, *76*, 1759-1763
[4] M. Moreno, W. Morris, M. G. Alvarez, G. S. Duffo, Corros. Sci., **2004,** *46*, 2681-2699
[5] J. L.Pandey, M. K. Banerjee, Anti-Corros. Method., **1998**, *45*, 5-15
[6] A. M. G. Seneviratne, G. Sergi, C. L. Page, Constr. Build. Mater., **2000**, *14*, 55-59
[7] D. G. Manning, Constr. Build. Mater., **1996**, *10*, 349-365
[8] J. J. Assaada, C. A. Issa, Constr. Build. Mater., **2012**, *30*, 667-674
[9] C. L. Page, G. Sergi, J. Mater. Civ. Eng., **2000**, *12*, 8-15
[10] T. A. Söyleva, M. G. Richardson, Constr. Build. Mater., **2008**, *22*, 609-622
[11] K. Y.Ann, H. S. Jung, H. S. Kim, Cem. Concr. Res., **2006**, *36*, 530-535
[12] J. F. Mike, J. L. Lutkenhaus, J. Polym. Sci., Part B: Polym. Phys., **2013**, *51*, 468-480
[13] A. Ramanavičius, A. Ramanavičiene, A. Malinauskas, Electrochim. Acta, **2006**, *51*, 6025-6037
[14] G. A. Snook, P. Kao, A. S. Best, J. Power Sources, **2011**, *196*, 1-12
[15] H. R. Tantawy, A. T. Weakley, D. E. Aston, J. Phys. Chem., **2014**, *C 118*, 1294-1305
[16] W. Feng, A. S. Wan, E. Garfunkel, J. Phys. Chem., **2013**, *C 117*, 9852-9863
[17] E. Ngaboyamahina, H. Cachet, A. Paillleret, E. M. M Sutter, Electrochimi. Acta, **2014**, *129*, 211-221
[18] N. C. T. Martins, T. Moura e Silva, M. F. Montemor, J. C. S. Fernandes, M. G. S. Ferreira, Electrochim. Acta, **2010**, *55*, 3580-3588
[19] N. C. T. Martins, T. Moura e Silva, M.F. Montemor, J. C. S. Fernandes, M. G. S. Ferreira, Electrochim. Acta, **2008**, *53*, 4754-4763
[21] H. Nguyen Thi Le, B. Garcia, C. Deslouis, J. Appl. Electrochem., **2002**, *32*, 105-110
[22] J. L. Camalet, J. C. Lacroix, S. Aeiyach, K. I. Chane-Ching, P. C. Lacaze, J. Electroanal. Chem., **1996**, *416*, 179-182.
[22] B. Wessling, Synth. Met., **1998**, *93*, 143-154
[23] K. M. Cheung, D. Bloor, G.C Stevens, J. Mater. Sci., **1990**, *25*, 3814-3837
[24] M. Bazzaoui, J. I. Martins, E. A. Bazzaoui, A. Albourine, L. Martins, Mater. Corros., **2014**, *65*, 67-75
[25] I. L. Lehr, S. B. Saidman, Corr. Sci., **2007**, *49*, 2210-2225
[26] Z. Zhang, M. Wan; Synth. Met., **2002**, *128*, 83-89
[27] S. R. Moraes, D. Huerta-Vilca, A. J. Motheo, Prog. Org. Coat., **2003,** *48*, 28-33
[28] G. Mengoli, M. M. Musiani, Electrochim. Acta., **1986**, *31*, 201-210
[29] J. L. Camalet, J. C. Lacroix, K. Chane-ching, S. Aeiyach, P. C. Lacaze, Synth. Met., **1993**, *93*, 133-142
[30] C. Q. Cui, L. H. Ogn, T. C. Tan, J. Y. Lee, Electrochim. Acta, **1993**, *38*, 1395-1404
[31] E. M.Genies, A.nBogly, M. Lapkowsky, C. Tsintavis, Synth. Met., **1990**, *36*, 139-182
[32] Q. G. Wang, N. J. Liu, X. H. Wang, J. Li, X. Zhao, F. Wang, Macromolecules, **2003,** 36, 5760-5764
[33] Q. Yu, J. Liu, J. Xu, Y. Yin, Y. Han, B. Li, J. Sol-Gel Sci. Tech., **2015**, *75,* 74-81
[34] L. Wei, Q. Chen, Y. Gu, Synth. Met., **2010**, *160*, 405-408
[35] M. Kazemi, I. Danaee, D. Zaarei, Mat. Chem. and Phys., **2014**, *148*, 223-229
[36] S. S. Pathak, A. S. Khanna, Prog. Org. Coat., **2008**, *62*, 409-416
[37] M. Mrad, M. F. Montemor, L. Dhouibi, E. Triki, Prog. Org. Coat., **2012,** *73*, 264–271
[38] E. Hur, G. Bereket, Y. Sahin, Prog. Org. Coat., **2006**, *57*, 149-158
[39] A.T. Ozyilmaz, Sur. Coat. Technol., **2006**, *200*, 3918-3925
[40] E. Kang, K. Neoh, K. Tan, Prog. Poly. Sci., **1998**, *23*, 277-324
[41] A. Pud, G. S. Shapoval, P. Kamarchik, N. Ogustov, V. F. Gromovaya, I. E. Myronyk, Y. V. Konstur, Synth. Met., **1999**, *30*, 111-115
[42] G. M. Spinks, A. J. Dominis, G. G. Wallace, D. E. Tallman, J. Sol. Stat. Electrochem., **2002**, *6*, 85-100
[43] P. J. Kinlen, D. C. Silverman, C. R. Jeffreys; Synth. Met., **1997**, *85*, 1327-1332
[44] W. K. Lu, B. Wessling; Synth. Met., **1995**, *71*, 2163-2166
[45] R. J. Holness, G. Williams, D. A. Worsley, H. N. McMurray; J. Electrochem. Soc., **2005**, *152*, B73-B81